Oxalate- and Ga^{3+}-Induced Structural Changes in Human Serum Transferrin and Its Recombinant N-Lobe. ^1H NMR Detection of Preferential C-Lobe Ga^{3+} Binding†

Gina Kubal,‡ Anne B. Mason,§ Sunil U. Patel,‡ Peter J. Sadler,*,‡ and Robert C. Woodworth§

Gordon House and Christopher Ingold Laboratories, Department of Chemistry, Birkbeck College, University of London, 29 Gordon Square, London WC1H 0PP, U.K., and the Department of Biochemistry, University of Vermont College of Medicine, Burlington, Vermont 05405

Received October 7, 1992; Revised Manuscript Received January 12, 1993

ABSTRACT: (1) The binding of the synergistic anion oxalate and Ga^{3+} to human serum transferrin (HTF, 80 kDa) and its recombinant N-lobe (HTF/2N, 40 kDa) has been studied by one- and two-dimensional ^1H NMR spectroscopy, at 310 K, pH* 7.25. (2) Specific protein resonances are sensitive to oxalate binding (fast exchange on the NMR time scale) and allowed determination of the apparent binding constant for oxalate binding to the N-lobe (log K 4.04). (3) Slow exchange between apo-HTF and Ga-loaded HTF or HTF/2N was observed. Binding of Ga^{3+} appeared to be accompanied by small changes in the orientations of residues in hydrophobic pockets in the interdomain hinge region close to the metal binding site. (4) Under the conditions used, preferential binding of Ga^{3+} (added as $Ga(NTA)_2$) to the C-lobe of HTF was observed. Binding to the C-lobe markedly perturbed resonances in the glycan *N*-acetyl region of the spectrum, suggesting that metal binding is communicated to the surface of the protein. This could be important in receptor recognition of metallotransferrins. (5) The displacement of Ga^{3+} from Ga-ox-HTF with Fe^{3+} was studied, and the paramagnetic broadening effects allowed identification of resonances from groups close to Fe^{3+}. The passage of Fe^{3+} from the exterior to the interior of the protein was followed by ^1H NMR spectroscopy, and the half-life for Ga^{3+}–Fe^{3+} exchange was determined to be 4.3 h (310 K).

Serum transferrin is an 80 kDa glycoprotein which delivers Fe^{3+} to cells via receptor-mediated endocytosis (Dautry-Varsat, 1986). The single chain protein consists of two structurally-similar lobes (40 kDa each) connected by a short peptide, each of which contains a metal binding site (Chasteen & Woodworth, 1990; Aisen, 1989; Harris & Aisen, 1989). Only the C-lobe is glycosylated (biantennary chains at Asn 413 and Asn 611; MacGillivray et al., 1983). The X-ray crystal structures of rabbit serum transferrin (Bailey et al., 1988; Sarra et al., 1990), and the related protein lactoferrin (Anderson et al., 1987, 1990), show that the Fe^{3+} in each lobe has approximate octahedral coordination from 2 Tyr oxygens, 1 His nitrogen, 1 Asp oxygen, and 2 oxygens from a bidentate carbonate anion. Metal ions cannot bind strongly in this site without concomitant binding of a synergistic anion.

There is much interest in the structural changes which accompany anion and metal ion binding that lead to receptor recognition of iron-loaded transferrin. For lactoferrin there is evidence that the metal-free N-lobe adopts an open conformation and that metal binding is accompanied by a closure of the cleft between the two domains which form the lobe (Anderson et al., 1990). Recent results from low-angle X-ray scattering have shown that both the N- and C-terminal lobes open on loss of Fe^{3+} from human transferrin and lactoferrin (Grossman et al., 1992).

In this work, we have investigated the binding of the synergistic anion oxalate and Ga^{3+} to human serum transferrin and to its recombinant N-lobe using high resolution ^1H NMR spectroscopy. Ga^{3+} is known to bind strongly to transferrin (Harris & Pecoraro, 1983; Valcour & Woodworth, 1987). It has a six-coordinate ionic radius (62 pm) similar to that of Fe^{3+} (65 pm; Shannon & Prewitt, 1969) and has the advantage of being diamagnetic, whereas Fe^{3+} is paramagnetic and broadens NMR resonances. There is pharmacological interest in Ga-HTF[1] since ^{67}Ga is an effective radiotracer used in diagnostic medicine (Parker, 1990).

^1H NMR studies on HTF are hampered by the large natural line widths which make individual resonances difficult to resolve. We have recently shown that this situation can be improved with the aid of certain resolution enhancement techniques and were able to follow sequential binding of Al^{3+} to the N- and C-lobes of HTF at pH* 8.8 with carbonate as the synergistic anion (Kubal et al., 1992a,b). Moreover, it appeared that some high-field-shifted methyl resonances could be reasonably assigned on the basis of ring current calculations. Some of these residues are in hydrophobic patches and may be intimately involved in hinge-bending processes which accompany domain closure on metal binding. In the present work, we show that ^1H NMR spectroscopy can be used to investigate the structural changes which accompany metal loading in the reverse order, i.e., C-lobe followed by N-lobe, and also that anion binding constants can be determined from NMR data. The role of the glycan chains in metal binding was also investigated.

† This research was supported by grants from the Science and Engineering Research Council, Medical Research Council, Wolfson Foundation and USPHS (Grant DK21739).

* To whom correspondence should be addressed.

‡ Birkbeck College, University of London.

§ University of Vermont College of Medicine.

[1] Abbreviations: COSY, homonuclear shift-correlated spectroscopy; DQF-COSY, double-quantum-filtered COSY, HTF, human serum transferrin; HTF/2N recombinant N-lobe of human serum transferrin (residues 1–337); LF, lactoferrin; NOESY, nuclear Overhauser effect spectroscopy; NTA, nitrilotriacetate; pH*, pH meter reading in D_2O solutions; RTF, rabbit serum transferrin; TSP, sodium trimethylsilyl-d_4-propionate.

0006-2960/93/0432-3387$04.00/0

MATERIALS AND METHODS

Materials. Apo-HTF was purchased from the Sigma Chemical Co. (catalog no. T0519, batch 67F9454). Recombinant HTF/2N (residues 1–337) was expressed in baby hamster kidney cells using a pNUT plasmid and purified as previously described (Funk et al., 1990). Iron was removed by treatment with NTA (1 mM) in 0.5 M sodium acetate, pH 4.9, followed by concentration in a Centricon 10 ultrafilter (Amicon). Potassium oxalate (ACS reagent) was purchased from Aldrich.

Stock solutions of Ga^{3+} were prepared by dissolution of $Ga(ClO_4)_3$ in D_2O and from gallium atomic absorption standards (1000 ppm, in 5% HNO_3, Johnson Matthey, in 1 wt % HNO_3, Aldrich), by addition of 2 mol equiv of H_2NTA (Aldrich) and pH adjustment to 6.2 with NaOD, to give a solution referred to as $Ga(NTA)_2$.

Prior to NMR experiments, apo-HTF and HTF/2N were dissolved in 0.1 M KCl in D_2O, the pH* was adjusted to 7.25, and the samples were left for 4 h at room temperature to allow H–D exchange before lyophilization. Samples were then redissolved in D_2O and the pH* was readjusted to 7.25 ± 0.05 when necessary using 0.1 M solutions of NaOD and DCl. Microliter aliquots of a stock solution of $K_2C_2O_4$ (0.1 M in D_2O), used as the synergistic anion, were added to 0.9 mM and 1.5 mM solutions of the apo-HTF and apo-HTF/2N, respectively. Protein concentrations were determined using ϵ_{280} values of 9.23×10^4 M^{-1} cm^{-1} (Luk, 1971) and 38.6 mM^{-1} cm^{-1} (Funk et al., 1990) for apo-HTF and apo-HTF/2N, respectively.

The pH* values of NMR solutions were recorded before and after NMR measurements using a micro-combination electrode (Aldrich) and a Corning 145 pH meter calibrated using pH 4, 7, and 10 buffers (Aldrich). Additions of Ga^{3+} as either $Ga(ClO_4)_3$ or $Ga(NTA)_2$ were made to HTF and HTF/2N samples containing oxalate with an average time of 0.5 h between additions. The pH* of each sample was adjusted to 7.25 ± 0.05. Iron was added to the Ga-HTF/2N sample as $Fe(NTA)_2$ (pH* 6.5, prepared from an iron atomic absorption standard, Johnson Matthey).

NMR Spectra. The 500-MHz ^1H NMR spectra were recorded on a Bruker AM500 spectrometer (Biomedical NMR Centre, National Institute for Medical Research, Mill Hill). Spectra were normally acquired using 0.45–0.55 mL of solution in a 5-mm tube at 310 K, with 256–512 transients, 45° pulses, a relaxation delay of 2 s, 8K data points (zero-filled to 16K), and gated secondary irradiation of HOD. The chemical shift reference used was either dioxan (3.764 ppm relative to TSP at 0 ppm) or endogenous formate (8.465 ppm, pH* > 7), which was always present in our samples as a minor impurity. Resolution enhancement of 1D spectra was achieved by processing the FID's with a combination of unshifted sine-bell functions and exponential functions equivalent to line broadenings of 1.5–20 Hz (Sadler & Tucker, 1992).

Two-dimensional phase-sensitive double-quantum-filtered COSY and NOESY spectra were obtained on a Varian Unity 600-MHz spectrometer (Biomedical NMR Centre, National Institute for Medical Research, Mill Hill), using 0.7 mL of solution in a 5-mm tube, 310 K. Typically, 200 increments of t_1 with 160 transients per increment were used with a relaxation delay of 1.75 s and a spectral width of 8000 Hz in both dimensions. Phase-sensitive DQF-COSY spectra were acquired using the hypercomplex method (States et al., 1982), and for the 2D NOESY spectrum, a mixing time of 50 ms was used. Shifted Gaussian functions were used in both dimensions for processing 2D spectra.

Binding and Rate Constants. The apparent binding constant for oxalate interacting with HTF/2N was determined from a Hill plot (Folajtar & Chasteen, 1982) of $-\log\{x/(1-x)\}$ versus $-\log$ [oxalate], where x is the fractional saturation. The kinetic parameters for the exchange of Ga^{3+} by Fe^{3+} in HTF/2N were determined from the rate of decrease in the height of peak B′ (Figure 6A) using the appropriate equation for pseudo-first-order kinetics (Atkins, 1982). Fits to the data were made using regression analysis and the program Kaleidagraph (Synergy Software, Reading, PA).

RESULTS

First we studied the effect of oxalate on the ^1H NMR spectrum of HTF/2N at pH* 7.25. Six additions of oxalate were made up to a total of 4.84 mol equiv. Oxalate had very little effect on peaks in the aliphatic or His C2H regions of the spectrum (Figure 1). For example, peak B shifts to low field by 0.01 ppm, two peaks merge into H_1, and the peak at 0.343 ppm shifts to 0.361 ppm. Most notable was the progressive high-field shift of a relatively sharp singlet at 5.994 ppm, peak S in Figure 2A. This is indicative of fast exchange of HTF/2N between free and oxalate-bound forms. The titration curve was fitted to a Hill plot (Figure 2B), giving an apparent binding constant of log K 4.04 ± 0.09 (R = 0.999), with a Hill coefficient of 1.3.

Additions of Ga^{3+}, as $Ga(NTA)_2$, were made (0.24, 0.45, 0.69, 0.87, and 0.99 mol equiv) to the above solution of HTF/2N containing 4.84 mol equiv of oxalate (ox-HTF/2N). In this case, specific resonances in both high- and low-field regions of the spectrum progressively disappeared while new resonances appeared, indicative of strong Ga^{3+} binding and slow exchange between ox-HTF/2N and Ga-ox-HTF/2N on the ^1H NMR chemical shift time scale. For example, high-field-shifted peaks A, B, and D for ox-HTF/2N gradually decrease in intensity and new peaks A′, B′, and D′ appear (Figure 1A). Similar peaks in the spectrum of Ga-ox-HTF/2N gave rise to clear connectivities in 2D COSY and DQF-COSY spectra (Figure 3 and Table I). Peaks B′ and B_1′ and H′ and H_1′ form pairs assignable to Val/Leu geminal methyls. We have tentatively assigned these peaks to Leu 122 and Val 246, respectively, on the basis of ring current calculations (Kubal et al., 1992b), together with that of peak A′ to the δCH_3 of Ile 132. Leu 122 and Ile 132 lie below and above the plane of the indole ring of Trp 128, and Val 246 is above Tyr 95, a metal ligand. These hydrophobic patches show a high degree of conservation in transferrins and lactoferrins. Comparisons of peak intensities and line widths in 1D spectra and connectivity patterns in 2D COSY spectra of ox-HTF/2N and Ga-ox-HTF/2N enable some reasonable correspondences to be made between peaks in the apo and Ga-loaded forms, e.g., B and B′, A and A′ (Table I). Notable shifts induced by Ga^{3+} complexation are those for peak A, 0.28 ppm to high field, peak D, 0.12 ppm to lower field, and peak B_1 0.11 ppm to high field.

In the His C2H region (Figure 1B), peaks L, N, and P decrease in intensity, and new peaks I′, J′, K′, M′, P′, Q′, and R′ appear. Peaks Q′ and R′ have notably very low-field shifts (8.164 and 8.709 ppm, respectively), and in an earlier study (Valcour & Woodworth, 1987) the latter had a pH-independent shift. When Ga^{3+} binds to ox-HTF/2N, peak S, which is sensitive to oxalate, decreases in intensity and disappears when the protein is fully-loaded, possibly appearing as the new peak T′ or broader peak S′ (Figure 2).

A NOESY spectrum of Ga-ox-HTF/2N was also recorded. This was complicated due to the very large number of

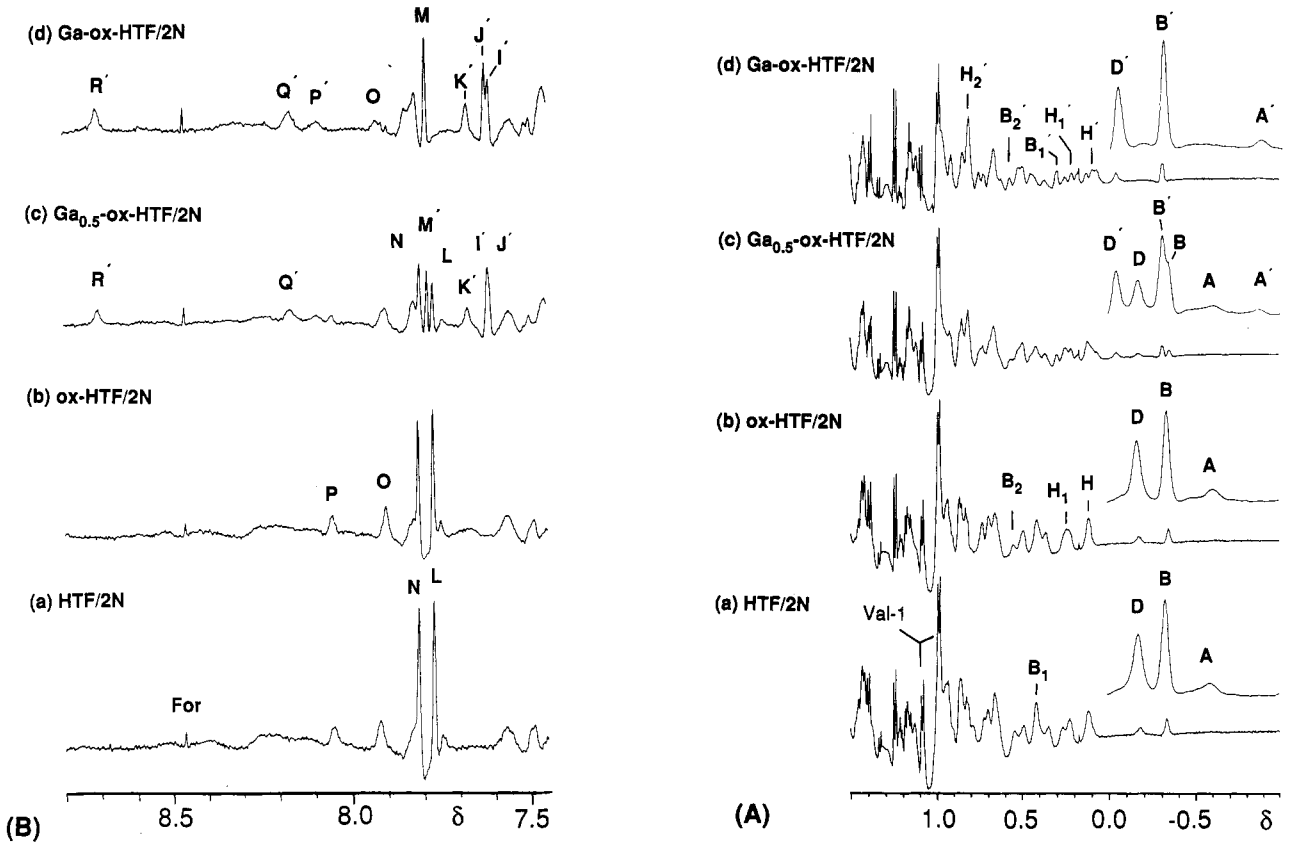

FIGURE 1: Resolution-enhanced 500-MHz ^{1}H NMR spectra of (A) the high-field region and (B) the histidine C(2)H region of apo-HTF/2N (1.5 mM) in 0.1 M KCl, pH* 7.25: (a) before and (b) after the addition of 4.84 mol equiv of oxalate, (c) after further addition of 0.45 mol equiv of Ga^{3+} (as $Ga(NTA)_2$), and (d) further addition of Ga^{3+} to a total of 0.99 mol equiv. A line-broadening function of 1.5 Hz combined with a sine-bell function was used for processing, except for the high-field inserts for which 20 Hz was used. Peaks which appear after Ga^{3+} addition are labeled with a prime (e.g., A'). Primed and nonprimed peaks with the same letter (e.g., B and B') may arise from the same spin system, but only in a few cases has further evidence for this been obtained (see Table I). The small sharp peak at 0.168 ppm is due to an impurity (probably grease).

overlapping cross-peaks and cannot be fully analyzed without further work. One region is very clearly resolved, that involving peak A' (previously assigned to δCH_3 of Ile 132; Kubal et al., 1992b) (Figure 3). This has associated cross-peaks at 0.151, 0.412, 0.868, and 1.324 ppm, consistent with intramolecular NOE's for an Ile spin system.

ox-HTF/2N was also titrated with $Ga(ClO_4)_3$. This gave rise to NMR spectra almost identical to those obtained with $Ga(NTA)_2$ additions.

Next, we studied the intact protein HTF. Enough oxalate (10.8 mol equiv) was added to ensure that full loading of the protein would occur on subsequent addition of Ga^{3+}. A detailed titration with oxalate was not carried out. In the aliphatic and His C2H regions, oxalate causes only minor changes in resonances, most notable is the apparent shift of peak O from 6.038 to 5.949 ppm (Figure 4B). Ga^{3+} was added as $Ga(NTA)_2$ in steps of 0.65, 1.30, 1.96, and 2.61 mol equiv with respect to protein. In the high-field region (Figure 4A) peaks a, e, g, and h appear to remain unchanged throughout the titration. Peak b decreases slightly in intensity, and a broad shoulder (b') appears at –0.297 ppm on addition of the second equivalent of Ga^{3+}, together with peak b_1' (Figure 4A). Peaks c and d decrease and increase in intensity, respectively, on addition of the first equivalent of Ga^{3+}, and both remain unchanged on addition of the second equivalent. In previous work with Al^{3+}, peak c was assigned to the C-lobe (Kubal et al., 1992a,b). Peak f' appears on addition of the second equivalent of Ga^{3+}. Peaks i and j both decrease in intensity on addition of the first equiv of Ga^{3+}, but whereas the former remains the same on addition of the second equiv of Ga^{3+}, peak j continues to decrease in intensity. Changes are also observed in the Lys/Arg region on addition of Ga^{3+} and in other parts of the aliphatic region (marked x in Figure 4A). Peaks labeled x_1 were only affected by addition of the second equivalent of Ga^{3+}, whereas peaks x_2 were affected by the first equivalent.

Figure 4B shows the same region (5.65–6.45 ppm) as that in Figure 2B for the N-lobe. Peak p' gradually increases in intensity on addition of 0–2 mol equiv Ga^{3+}. Peak q decreases in intensity, and a new similar peak appears slightly to low field (q'; Figure 4B). This change occurs during addition of the first equiv of Ga^{3+}. This peak clearly illustrates the slow exchange (on the NMR time scale) of protein between apo and Ga-loaded forms.

In the His C2H region (Figure 4C), peaks s', t', z', and aa' appear on addition of the first equivalent of Ga^{3+} but remain unchanged with the second equivalent. Peaks x and bb decrease in intensity on addition of the first equivalent of Ga^{3+}, whereas peaks v and y decrease in intensity gradually throughout the titration. Peak w only decreases in intensity on addition of the second equivalent of Ga^{3+}. A new broad low-field peak, ff' (8.78 ppm), appears on addition of the first equivalent of Ga^{3+}, and peak dd disappears. There is also a new very broad peak ee' at 8.35 ppm, but it is difficult to assess when it first appears. Peak r and the peak for formate, for example, remain essentially unchanged throughout the titration.

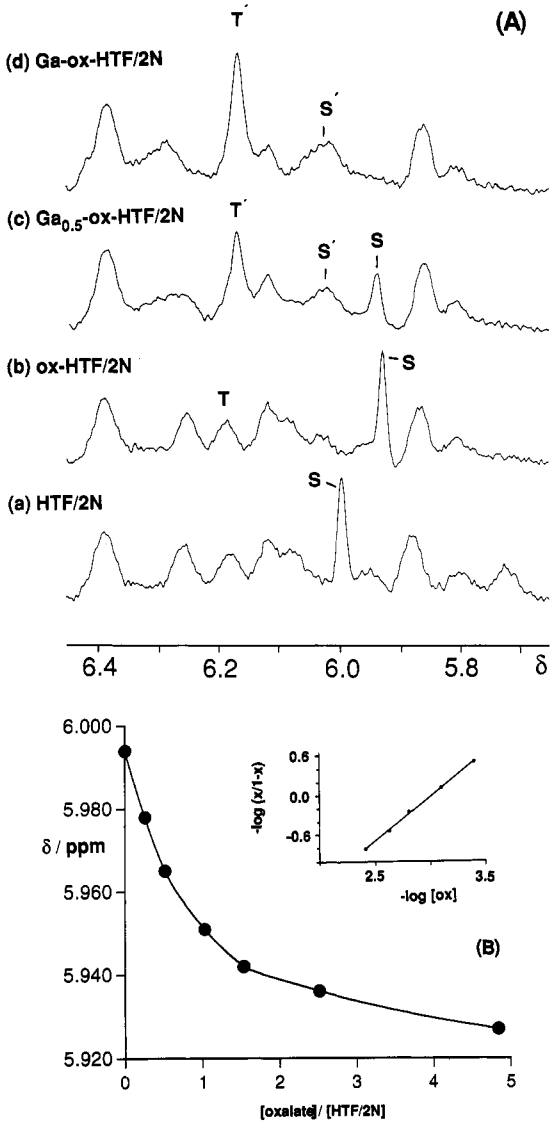

FIGURE 2: (A) Expansions of part of the aromatic region of the same spectra shown in Figure 1 (resolution enhanced, line broadening of 3 Hz): (a) Apo-HTF/2N, (b) +4.84 mol equiv oxalate, (c) + a further 0.45 mol equiv of Ga^{3+}, and (d) a total of 0.99 mol equiv of Ga^{3+}. (B) Dependence of the chemical shift of peak S on oxalate concentration and Hill plot (insert; slope is the Hill coefficient *n*, and the ordinate intercept –log *K*).

The *N*-acetyl/*S*-methyl (Met) region of the spectrum (Figure 5) does not change after addition of oxalate to HTF (or HTF/2N). In contrast, on addition of the first equivalent of Ga^{3+} to ox-HTF, a new apparent singlet appears progressively at 2.097 ppm and the peak at 2.08 ppm splits into two. No further changes occur in this region on addition of the second equivalent of Ga^{3+}. The peaks in this region of the spectrum of HTF are the most intense in the spectrum, suggesting that they belong to the very mobile *N*-acetyls of the four NAcGlc and two NAcNeu residues in each of the two glycan chains of HTF, although the peak at 2.132 ppm decreases in intensity on oxidation of HTF with H_2O_2 (G. Kubal and P. J. Sadler, unpublished) and is therefore probably a Met *S*-methyl peak. There are no analogous peaks in the 2.0–2.1 ppm region of the spectrum of the N-lobe, which does not contain glycan chains. Isolated glycopeptides from HTF are known to have NAc shifts in the range 2.01–2.09 ppm (Dorland et al., 1977). In the corresponding region of the spectrum for ox-HTF/2N (Figure 5), a singlet at 2.165 ppm, which could be a Met *S*-methyl peak, gradually disappears on titration with Ga^{3+}. No corresponding peak is seen for

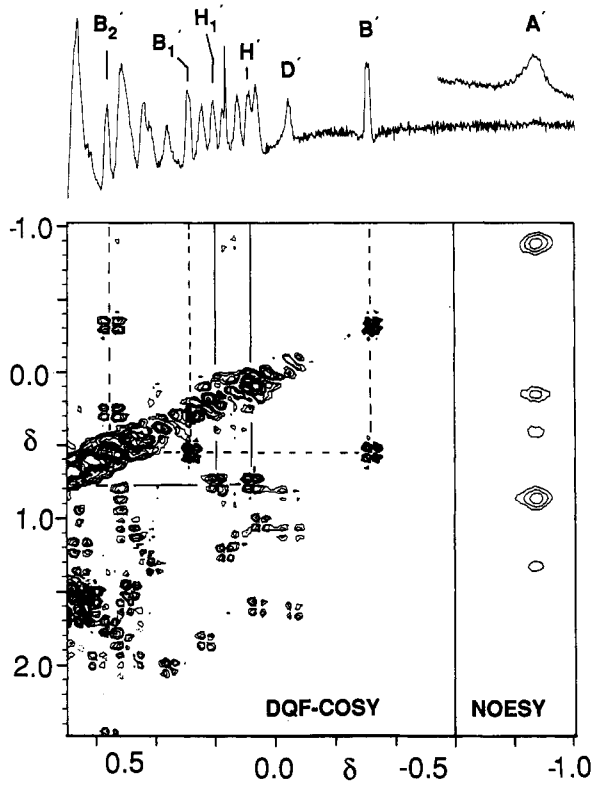

FIGURE 3: The 600-MHz phase-sensitive DQF-COSY ^1H NMR spectrum of the high-field region of Ga-ox-HTF/2N (1.53 mM apo-HTF/2N + 4.84 mol equiv of oxalate +1 mol equiv of $Ga(ClO_4)_3$, pH* 7.25), together with a NOESY spectrum for the highest field peak.

ox-HTF, presumably because it is too broad to observe. Only one of the five ^{13}C *S*-methyl peaks observed for ^{13}C-labeled HTF/2N is sensitive to Ga^{3+} binding to the protein: the second to lowest field ^{13}C peak disappears and is replaced by a new peak 1.5 ppm to higher field (Luck et al., 1993).

In an attempt to correlate resonances in the spectra of Ga-ox-HTF/2N with those for Fe-ox-HTF/2N, slightly less than 1 mol equiv of Fe^{3+} (to avoid excess free Fe^{3+}) was added as $Fe(NTA)_2$ to Ga-ox-HTF/2N. Fe^{3+} is known to bind to HTF/2N more tightly than Ga^{3+} (Harris & Pecoraro, 1983), and the time course of the reaction was followed for a period of 24 h by ^1H NMR spectroscopy. In the early stages of the reaction, resonances for small molecules such as formate (present as an impurity) and the mobile N- and C-terminal residues of the protein (Val 1 and Asp 337) were broadened, and those in the remainder of the spectrum (e.g., the high-field-shifted methyl resonances, 0 to –1 ppm) remained unchanged (Figure 6). At later times, specific broadening of other protein peaks occurred progressively with time, consistent with entry of paramagnetic Fe^{3+} into the interdomain site and displacement of Ga^{3+}. This was accompanied by a resharpening of the resonances for the most mobile protons. No further spectral changes were observed after 18 h. In the high-field methyl region, peaks A′, B′, and D′, which were sensitive to Ga^{3+} binding to ox-HTF/2N (Figure 1A) are noticeably broadened for Fe-ox-HTF/2N. Resonances assigned to Val 1 (N-terminal valine residue) and Asp 337 (C-terminal aspartate residue) are well-resolved multiplets in both the Ga-ox-HTF/2N and Fe-ox-HTF/2N. The singlet at 2.216 ppm (a possible *S*-methyl resonance) broadened slightly on addition of Fe^{3+} and remained broadened throughout the reaction. In the aromatic region, the most broadened peaks for Fe-ox-HTF/2N are I′, J′, K′, N′, Q′, and R′, the latter most likely being assignable to His 249, a metal ligand.

Table I: Chemical Shifts for ^{1}H NMR Resonances of HTF/2N and Its Oxalato, Ga^{3+}, and Al^{3+} Complexes[a]

protein	(Leu 122) B	B_1	B_2	(Val 246) H	H_1	H_2	(Ile 132) A	(?) D
HTF/2N	−0.333	0.418	0.542	0.119	0.223	0.824	−0.605	−0.173
ox-HTF/2N	−0.343	0.412	0.548	0.118	0.228	0.828	−0.617	−0.166
Ga-ox-HTF/2N	−0.308	0.299	0.567	0.089	0.210	0.812	−0.897	−0.044
$\Delta\delta$(Ga)[b]	0.035	−0.113	0.019	−0.029	−0.018	−0.016	−0.280	0.122
CO_3-HTF/2N[c]	−0.333						−0.635	−0.110
Al-CO_3-HTF/2N[c]	−0.401	0.346	0.512	0.095	0.212	0.818	−0.839	−0.042
$\Delta\delta$(Al)[b]	−0.068						−0.204	0.068

[a] Connectivities were obtained from COSY and DQF-COSY spectra, and assignments are based on ring current calculations (Kubal et al., 1992). Peak labels are shown in Figure 1. [b] Coordination shifts. [c] Data from Kubal et al. (1992b).

The decrease in height of peak B′ (Figure 6A) with time followed pseudo-first-order kinetics and, from the linear plot of ln (A_t/A_0) versus time (where A_t and A_0 are the peak heights at time t and time zero, respectively; $R = 0.996$), a rate constant k_{obs} of 0.162 ± 0.004 h^{-1} was determined giving a half-life for Ga^{3+}–Fe^{3+} exchange of 4.29 h.

DISCUSSION

We have investigated the binding of Ga^{3+} to intact HTF and its recombinant N-lobe in the presence of the synergistic anion oxalate. The natural synergistic anion is thought to be carbonate in blood (Anderson et al., 1987, 1990; Bailey et al., 1988; Sarra et al., 1990), but in vitro the carbonate/CO_2 equilibrium is difficult to maintain at lower pH's. Ga^{3+} has a similar ionic radius to Fe^{3+} and is known to bind to HTF with a similar equilibrium behavior. It has the advantage of being diamagnetic whereas bound Fe^{3+} is high-spin with five unpaired electrons and broadens NMR resonances (vide infra). At the pH* used for our experiments, 7.25, oxalate (pK_a's 1.04 and 3.55; Martell & Smith, 1977) exists as a dianion and there is interest in the possibility that such synergistic anions preform the interdomain clefts of transferrins to lower the activation energies for metal binding (Anderson et al., 1990).

We have recently shown that ^{1}H NMR spectroscopy can be used to determine the order in which the lobes of intact HTF are loaded by first identifying features in the spectrum of the recombinant N-lobe which are sensitive to metal binding and then attempting to find matching features in spectra of HTF (Kubal et al., 1992b). Both HTF and HTF/2N are large proteins for high-resolution ^{1}H NMR spectroscopy and only a fraction of the total number of resonances can be resolved in 1D and 2D spectra on account of their broadness and the extensive overlap. However, this procedure is aided by the use of certain resolution enhancement techniques and appeared to be successful for Al^{3+} loading. Moreover, it appeared that resolvable resonances do not merely arise from mobile unstructured regions of the protein but that some belong to mobile structured hydrophobic patches.

This comparative approach to the determination of the order of lobe loading depends on several assumptions. First the structure of the N-lobe and its loading characteristics are similar in HTF/2N and HTF. This is a reasonable assumption since the X-ray structure of Fe-RTF/2N (rabbit) is almost identical to that of the N-lobe in Fe_2-RTF (Sarra et al., 1990; Bailey et al., 1988), although the apoproteins are likely to be much more flexible. Second, loading of one lobe does not cause major changes in the structure of the other lobe (i.e., little interlobe communication), and third, peaks in the spectrum of HTF which are sensitive to metal (or anion) binding can be uniquely assigned to one lobe, and any overlap of resonances can be interpreted. Two-dimensional spectra can aid the latter problem, although 2D spectra of HTF (usually <1 mM) give rise to very weak cross-peaks and currently are not routinely useful. Situations could also occur in which the binding constants and kinetics for both sites are similar and so both load together. Eventually it is hoped that NMR will be useful for distinguishing between all the various possibilities.

Despite the potential limitations of the procedure, our data clearly suggest that under the conditions used (pH* 7.25, 0.1 M KCl, oxalate as synergistic anion, and $Ga(NTA)_2$ as loading agent), Ga^{3+} preferentially loads the C-lobe followed by the N-lobe, in contrast to our previous findings with Al^{3+} (pH* 8.8, HCO_3^- as synergistic anion), which entered the N-lobe first. For both Al^{3+} and Ga^{3+}, separate resonances are seen for free HTF or HTF/2N and their metal-bound forms. Slow exchange behavior on the NMR time scale is characteristic of tightly bound metal ions.

In the high-field region of the spectrum of HTF, the resonances which we have tentatively assigned to Leu 122 (b, b_1, b_2) by analogy with HTF/2N (Kubal et al., 1992b), are perturbed only by the second equivalent of Ga^{3+}, whereas changes in the region where resonances from the *N*-acetyls of the glycan chains in the C-lobe are expected (2.0–2.1 ppm; Figure 5) occur on addition of the first equivalent of Ga^{3+}. There is a possibility that some of the apparent singlets in this *N*-acetyl region belong to the *S*-methyl groups of the four Met residues of the C-lobe. By analogy with the structure of Fe_2-RTF (Bailey et al., 1988), two of these (Met 389 and 464) are buried (and are therefore likely to give broad peaks), one is partially buried (Met 498), and only one (Met 382) is in a highly mobile surface environment. Met 464 is an interesting residue because it occupies an analogous position to Ile 132 in the N-lobe, part of the Trp 128 (Trp 460 in C-lobe) hydrophobic patch. The *S*-methyl group is within 3–5 Å of the faces of the aromatic rings of Trp 460 and Phe 476, and therefore likely to be well shifted to high field. The biantennary glycan chains in HTF are attached to Asn 413 and Asn 611. In crystals of Cu_2-LF (and Fe_2-LF) the glycan chains are very mobile and give only weak electron density, although the first NAcGlc sugar residue, which is covalently bound to Nδ_2 of Asn 137 in the N-lobe of Cu_2-LF, forms hydrogen bonds to Glu 110 and a solvent water molecule (Smith et al., 1992). In the present case, Ga^{3+} binding may lead to a change in the local structure associated with the N-acetylated sugar residues of the biantennary chains at either Asn 413 or Asn 611 and the surface structure of the protein. In this way communication between the metal site and the protein surface could be established. This effect was not observed in our previous Al^{3+} experiments (Kubal et al., 1992). In crystalline Fe_2-RTF, the glycan chain at Asn 491 bridges the solvent region between the N- and C-lobes (Bailey et al., 1988). The disappearance of peak c in the spectrum of HTF

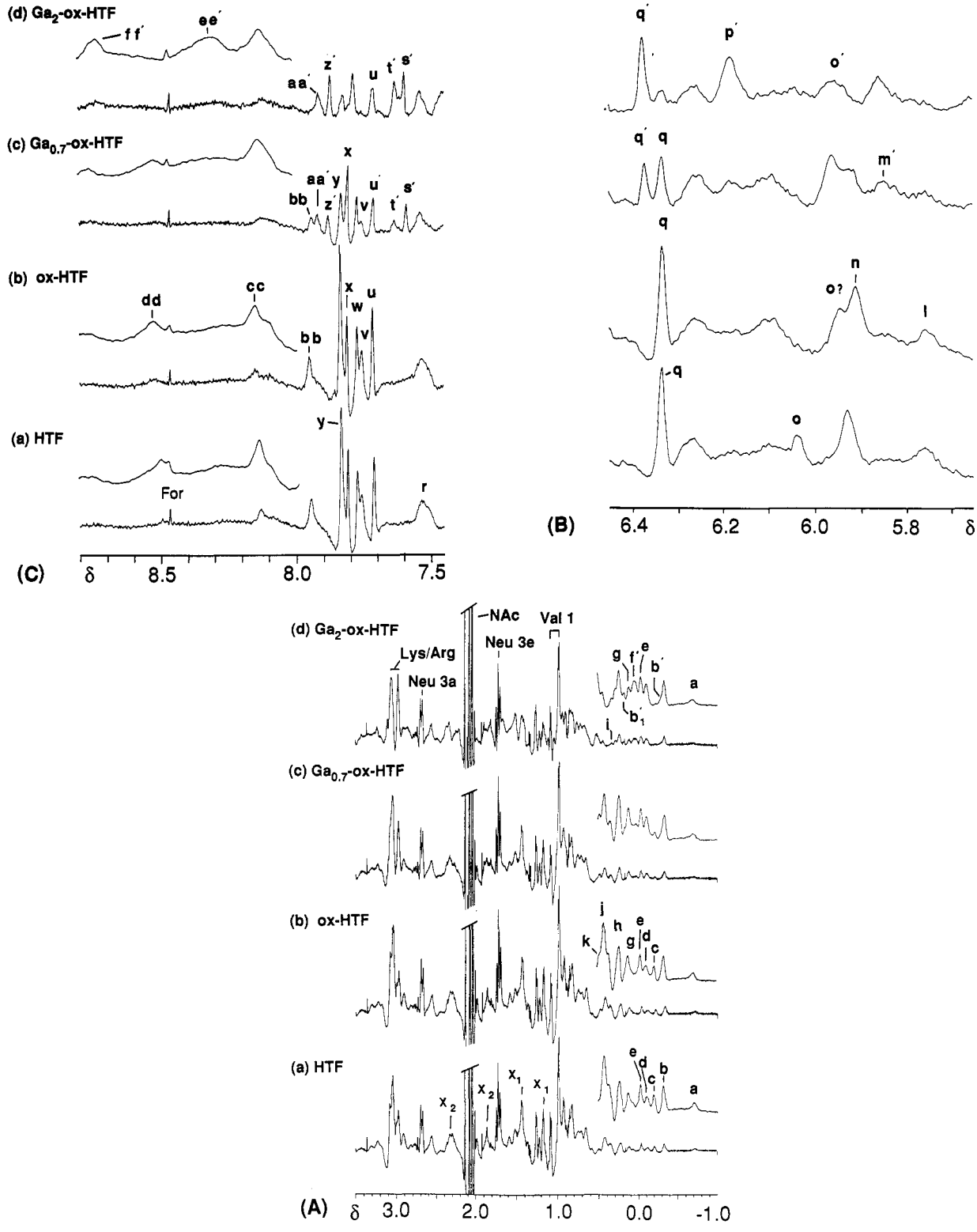

FIGURE 4: The 500-MHz ^{1}H NMR spectra of apo-HTF (0.9 mM) in 0.1 M KCl, pH 7.25: (A) Aliphatic region; (B and C) aromatic regions. Spectra: (a) before or (b) after addition of 10.8 mol equiv of oxalate, (c) further addition of 0.65 mol equiv of Ga^{3+} ($Ga(NTA)_2$), and (d) a total of 1.96 mol equivalents of Ga^{3+}. (The sharp peak at 0.168 ppm is due to an impurity.)

(Figure 4A) appears to be another useful indication of Ga^{3+} binding to the C-lobe.

Consideration of the aromatic region of HTF does not provide such convincing evidence for preferential loading of the C-lobe. In part this arises from the extreme sensitivity of many His C2H resonances to very small changes in pH* around the pH* chosen for this work (7.25). For our earlier work on Al^{3+}, we chose a pH* of 8.8 to avoid such complications. Two prominent new resonances appear at 8.164 (Q′) and 8.709 (R′) ppm on binding Ga^{3+} to the N-lobe (Figure 1B). The latter peak does not shift with pH* (Valcour & Woodworth, 1987) and is assignable to the C2H of His 249, a metal ligand. Similar, but broader, peaks appear to be present on adding the first equivalent of Ga^{3+} to HTF, and this might suggest that the N-lobe of HTF is loaded first. However, they intensify on adding the second equivalent of Ga^{3+}, perhaps because there is an analogous ligand, His 585, in the C-lobe. These low-field peaks were not seen for Al^{3+}

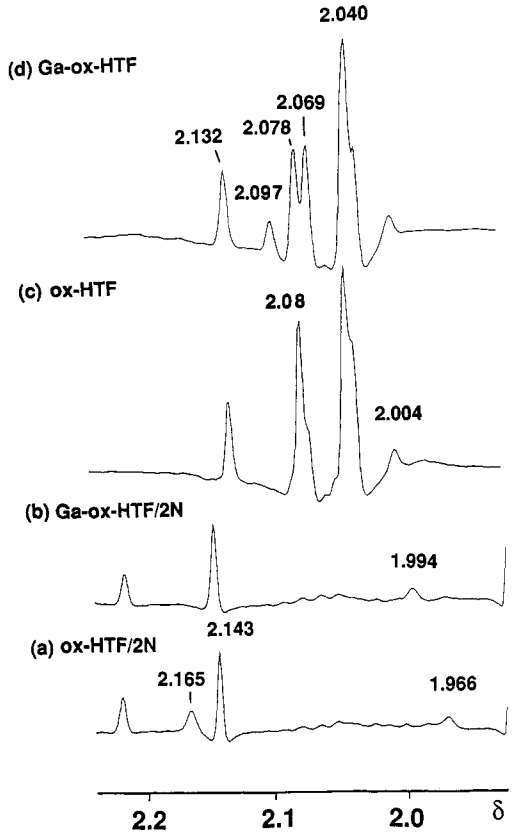

FIGURE 5: The 500-MHz ^{1}H NMR spectra of the *N*-acetyl and *S*-methyl regions of (a) HTF/2N + 4.84 mol equiv of oxalate (pH* 7.25), (b) after addition of 1 mol equiv of Ga^{3+} ($Ga(ClO_4)_3$), (c) HTF + 10.8 mol equiv of oxalate pH* 7.24, and (d) after addition of 1 mol equiv of Ga^{3+} ($Ga(ClO_4)_3$), pH* 7.20. Spectrum d remains almost unchanged on addition of a second mol equiv of Ga^{3+}. All samples contained 0.1 M KCl.

loading of HTF or HTF/2N (Kubal et al., 1992a,b), and it is reasonable to suppose that His 249 is not a ligand for Al^{3+} which is likely to have a lower affinity for N ligands than Fe^{3+} or Ga^{3+}.

The relatively sharp peak (q′) at 6.339 ppm provides a clear monitor of the binding of Ga^{3+} to HTF, apparently undergoing a small downfield shift (Figure 4B). Our pH titration of HTF (G. Kubal and P. J. Sadler, unpublished) shows that this peak has an associated pK_a of 5.87 and is probably assignable to a high-field-shifted His C4H, although its pH titration shift range (0.75 ppm) is unusually high (Gross & Kalbitzer, 1988). It might therefore be a very high-field-shifted C2 His proton, perhaps from a His residue lying close to the face of an aromatic ring of a nearby side chain. There does not appear to be a similar peak in spectra of the N-lobe.

Taken together, the data for Ga^{3+} binding to HTF at pH 7.25 with oxalate as the synergistic anion suggest that the C-lobe is populated first followed by the N-lobe. This is consistent with previous reports of loading HTF with Fe^{3+} under similar conditions (Harris & Aisen, 1989).

We have shown that it is possible to use ^{1}H NMR spectroscopy to determine the binding constants for anion binding to apo-HTF/2N. Previously, a variety of other methods have been used for this purpose (with HTF), including equilibrium dialysis, electrophoresis, chemical modification, EPR, and UV difference spectroscopy (Woodworth et al., 1975; Folajtar & Chasteen, 1982; Harris, 1985). The value we have determined for oxalate binding to HTF/2N (log *K* 4.04) is close to values reported previously for oxalate binding to HTF and close to values for the nonsynergistic anions phosphate and arsenate. Further insight into the nature of the binding site will be gained when assignments can be made for resonances perturbed by oxalate. Since oxalate has little effect on resonances we have assigned to hydrophobic patches around the cleft, it seems that oxalate does not completely preform the metal binding site. Oxalate binding is weak enough for fast exchange to be observed on the NMR time scale, consistent with low activation energies for the structural changes involved in oxalate binding, unlike those which accompany metal binding.

A detailed titration of HTF itself with oxalate was not carried out, but it appeared that specific peaks were sensitive to oxalate binding (Figure 4). For example, peak o (Figure 4B) which seemed to shift to high field on oxalate binding, may be the analogue of peak S of HTF/2N (Figure 1B) and therefore belong to the N-lobe of HTF. It may be possible to extend this work to the determination of anion binding constants for the individual lobes of HTF.

The displacement of Ga^{3+} by Fe^{3+} (added as an NTA complex) was very slow, taking about 18 h to reach completion at 310 K. There do not appear to be any previous reports of the kinetics of this reaction, which presumably requires a partial opening of the interdomain cleft, followed by ligand interchange reactions in the binding cleft. Kinetic barriers to metal removal are a well-known feature of transferrin biochemistry (Aisen & Listowsky, 1980) and may dominate its physiological properties. In the early stages of the Ga^{3+}–Fe^{3+} exchange reaction, it was clear from the NMR data that $Fe(NTA)_2$ binds weakly to low molecular mass ligands in the solution such as formate and acetate (impurities) and accessible protein groups such as the amino and carboxylato terminii. This weak binding (ternary or outer sphere) could play a role in the mechanism of Fe^{3+} uptake into the binding cleft. NMR spectroscopy may prove to be a useful new method for investigating the effect of mediators on metal-exchange reactions of transferrins.

Resonances in the spectrum of Fe-ox-HTF/2N which were broadened the most are likely to arise from protons nearest to Fe^{3+} (paramagnetic dipolar broadening, $\alpha 1/r^6$; Dwek, 1973) and were the same peaks as those which were shifted by Ga^{3+} binding to ox-HTF/2N. This implies similar modes of binding for Fe^{3+} and Ga^{3+} and provides further confirmation that the residues previously associated with peaks B′ and H′, Leu 122 and Val 245, respectively (Kubal et al., 1992b), are close to Fe^{3+}. It is interesting to compare the Al^{3+}- and Ga^{3+}-induced coordination shifts for resonances of HTF/2N tentatively assigned to Leu 122 and Ile 132 (Table I). These residues lie below and above Trp 128 in a hydrophobic patch in close contact with the anion and metal ion binding site. For both Al^{3+} binding with carbonate as synergistic anion a pH* 8.8, and Ga^{3+} binding with oxalate as anion at pH* 7.25, the δCH_3 of Ile 132 (peak A) moves closer into the shielding cone of Trp 128, but the small effect on $\delta_1 CH_3$ of Leu 122 (peak B) is opposite in the two cases. Ring current-induced shifts can be sensitive to atomic movements of <0.1 Å (Perkins, 1982) and may provide useful monitors of subtle structural changes within the interdomain cleft. However, further work is required to establish firm correspondences between resonances in spectra of apo- and Ga-transferrins (e.g., 2D phase-sensitive NOESY experiments) and to confirm the assignments to specific amino acid residues.

CONCLUSIONS

Transferrin is a flexible protein with strong metal binding sites located in interdomain clefts. It is important to

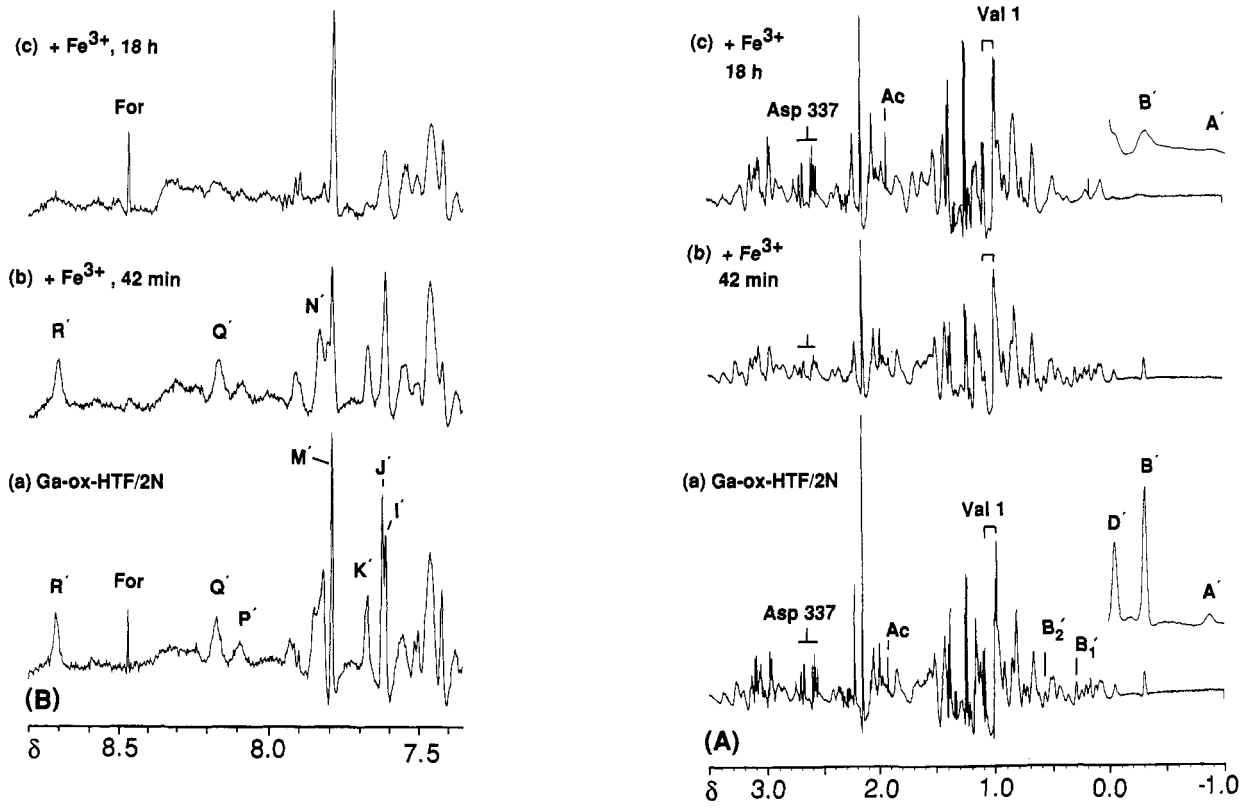

FIGURE 6: Resolution-enhanced 500-MHz ^{1}H NMR spectra of (A) aliphatic region and (B) aromatic region of (a) Ga-ox-HTF/2N (apo HTF/2N + 4.8 mol equiv of oxalate + 1 mol equiv of Ga^{3+} ($Ga(ClO_4)_3$), pH* 7.26), and (b) 42 min after addition of 0.84 mol equiv of Fe^{3+} (added as $Fe(NTA)_2$), and (c) after 18 h (equilibrium). In the early stages of the reaction, sharp resonances from mobile protons in surface regions of the protein are broadened, together with those for small metal binding ligands such as formate. In the later stages the latter resonances sharpen again as Fe^{3+} is taken into the interior site and resonances from nearby hydrophobic patches broaden.

understand the dynamic structural changes which accompany both anion and metal ion uptake and release and their role in iron delivery to cells via receptor-mediated endocytosis. Both transferrin (80 kDa) and its half molecule the N-lobe (40 kDa) are large molecules for high-resolution ^{1}H NMR studies, and only a small proportion of the total number of resonances is resolvable, even with harsh resolution enhancement techniques. However, the resolved peaks are not merely from unstructured mobile protons. They arise from His residues distributed over the protein, from mobile but structured hydrophobic patches in close contact with the metal site, and from other as yet unidentified residues which are sensitive to metal and anion binding.

We have shown that ^{1}H NMR spectroscopy can be used to determine the binding constants for anion binding to the N-lobe, but the procedure should be extendible to the intact protein. Oxalate binds relatively weakly to apo-HTF/2N (log K 4.04) but specifically, since only certain resonances are perturbed. Specific resonances are also perturbed by Ga^{3+} binding, which is strong, as reflected by slow exchange between apoproteins and Ga-loaded proteins on the NMR time scale. Low-field-shifted peaks assignable to protons of coordinated His were observed for Ga^{3+} complexes of both ox-HTF and ox-HTF/2N. The NMR data suggest that $Ga(NTA)_2$ preferentially loads the C-lobe at pH* 7.25 with oxalate as synergistic anion. The changes observed for resonances in the glycan N-acetyl region of the spectrum suggest that Ga^{3+} binding is communicated to the surface of the C-lobe, an event which could be important to receptor recognition of metallotransferrins. Apotransferrins are not recognized by the transferrin receptor at plasma pH.

It was possible to use paramagnetic broadening effects to determine the rate of exchange of Ga^{3+} in Ga-ox-HTF/2N with Fe^{3+} as $Fe(NTA)_2$ (k_{obs} 0.162 h^{-1}, 310 K). The slowness of the reaction appears to reflect the high activation barriers associated with the ligand exchange processes involved, including the opening of the interdomain cleft. Such kinetic control is likely to dominate the physiological behavior of transferrin.

These studies suggest that ^{1}H NMR spectroscopy can provide new insights into changes in structure and dynamics associated with both anion and metal binding to intact transferrins and recombinant lobes.

ADDED IN PROOF

Recent ^{13}C and ^{27}Al NMR studies have shown that the synergistic anion can determine the specificity of Al^{3+} binding to ovotransferrin:preferential uptake into the C-lobe with oxalate and the N-lobe with carbonate [Aramini, J. M., & Vogel, N. J. (1993) *J. Am. Chem. Soc. 115*, 245–252].

ACKNOWLEDGMENT

We thank Drs. T. A. Frenkiel and C. J. Bauer (Biomedical NMR Centre, Mill Hill) for advice and assistance with NMR measurements, Dr. A. Tucker (Birkbeck) and Dr. R. W. Evans (Guy's) for helpful discussions, and Dr. P. F. Lindley (Birkbeck) and Dr. E. N. Baker (Massay) for supplying coordinates of rabbit transferrin and human lactoferrin, respectively.

REFERENCES

Aisen, P. (1989) in *Iron Carriers and Iron Proteins* (Loehr, T. M., Ed.) pp 353–371, VCH Publishers Inc., New York.

Aisen, P., & Listowsky, I. (1980) *Annu. Rev. Biochem. 49*, 357–393.
Anderson, B. F., Baker, H. M., Dodson, E. J., Norris, G. E., Rumball, S. V., Waters, J. M., & Baker, E. N. (1987) *Proc. Natl. Acad. Sci. U.S.A. 84*, 1769–1773.
Anderson, B. F., Baker, H. M., Norris, G. E., Rumball, S. V., & Baker, E. N. (1990) *Nature 344*, 784–787.
Atkins, P. W. (1982) *Physical Chemistry*, 2nd ed., pp 920–968, Oxford University Press, Oxford.
Bailey, S., Evans, R. W., Garratt, R. C., Gorinsky, B., Hasnain, S., Horsburgh, C., Jhoti, H., Lindley, P. F., Mydin, A., Sarra, R., & Watson, J. L. (1988) *Biochemistry 27*, 5804–5812.
Chasteen, N. D., & Woodworth, R. C. (1990) in *Iron Transport and Storage* (Ponka, P., Schulman, H. M., & Woodworth, R. C., Eds.) pp 68–79, CRC Press, Boca Raton, FL.
Dautry-Varsat, A. (1986) *Biochemie 68*, 375–381.
Dorland, L., Haverkamp, J., Schut, B. L., Vliegenthart, J. F. G., Spik, G., Strecker, G., Fournet, B., & Montreuil, J. (1977) *FEBS Lett. 77*, 15–20.
Dwek, R. A. (1973) *Nuclear Magnetic Resonance in Biochemistry*, Clarendon Press, Oxford, England.
Folajtar, D. A., & Chasteen, N. D. (1982) *J. Am. Chem. Soc. 104*, 5775–5780.
Funk, W. D., MacGillivray, R. T. A., Mason, A. B., Brown, S. A., & Woodworth, R. C. (1990) *Biochemistry 29*, 1654–1660.
Gross, K.-L., & Kalbitzer, H. R. (1988) *J. Magn. Reson. 76*, 87–99.
Grossman, J. G., Neu, M., Pantos, E., Schwab, F. J., Evans, R. W., Townes-Andrews, E., Lindley, P. F., Appel, H., Thies, W.-G., & Hasnain, S. S. (1992) *J. Mol. Biol. 225*, 811–819.
Harris, D. C. (1985) *Biochemistry 24*, 7412–7418.
Harris, D. C., & Pecoraro, V. L. (1983) *Biochemistry 22*, 292–299.
Harris, D. C., & Aisen, P. (1989) in *Iron Carriers and Iron Proteins* (Loehr, T. M., Ed.) pp 239–351, VCH Publishers Inc., New York.
Kubal, G., Sadler, P. J., & Evans, R. W. (1992a) *J. Am. Chem. Soc. 114*, 1117–1118.
Kubal, G., Mason, A. B., Sadler, P. J., Tucker, A., & Woodworth, R. C. (1992b) *Biochem. J. 285*, 711–714.
Luck, L. A., Mason, A. B., MacGillivray, R. T. A., Savage, K., & Woodworth, R. C. (1993) *Protein Sci.* (submitted for publication).
Luk, C. K. (1971) *Biochemistry 10*, 2838–2843.
MacGillivray, R. T. A., Mendez, E., Shewale, J. G., Sinha, S. K., Lineback-Zins, J., & Brew, K. (1983) *J. Biol. Chem. 258*, 3543–3553.
Martell, A. E., & Smith, R. M. (1977) *Critical Stability Constants*, Vol. 3, p 92, Plenum Press, New York.
Parker, D. (1990) *Chem. Brit. 26*, 942–945.
Perkins, S. J. (1982) *Biol. Magn. Reson. 4*, 193–336.
Sadler, P. J., & Tucker, A. (1992) *Biochem. J. 205*, 631–643.
Sarra, R., Garratt, R., Gorinsky, B., Jhoti, H., & Lindley, P. F. (1990) *Acta Crystallogr. B46*, 763–771.
Shannon, R. D., & Prewitt, C. T. (1969) *Acta Crystallogr. B25*, 925–946.
Smith, C. A., Anderson, B. F., Baker, H. M., & Baker, E. N. (1992) *Biochemistry 31*, 4527–4533.
States, D. J., Haberkorn, R. A., & Ruben, D. J. (1982) *J. Magn. Reson. 48*, 286–292.
Valcour, A. A., & Woodworth, R. C. (1987) *Biochemistry 26*, 3120–3125.
Woodworth, R. C., Virkaitis, L. M., Woodbury, R. G., & Fava, R. A. (1975) in *Proteins of Iron Storage and Transport in Biochemistry and Medicine* (Crichton, R. R., Ed.) pp 39–50, North Holland Publishing Co.